PHYSICAL REVIEW A VOLUME 22, NUMBER 5 NOVEMBER 1980

Measurement of radiative lifetimes of low-lying excited states in sodiumlike, fluorinelike, and oxygenlike iron

J. P. Buchet, M. C. Buchet-Poulizac, A. Denis, J. Désesquelles, and M. Druetta
Laboratoire de Spectrométrie Ionique et Moléculaire, Université de Lyon I, Campus de la Doua, 69622-Villeurbanne Cedex, France
(Received 10 April 1980)

We have used the beam-foil technique to study the spectra of Fe XVI to Fe XX ions in the far vacuum ultraviolet range and to measure the mean lives of the upper levels of the $3s$-$3p$ and $3p$-$3d$ transitions in sodiumlike Fe XVI, the $2s^2 2p^5\ ^2P^o_{3/2} - 2s 2p^6\ ^2S_{1/2}$ resonance transition in F-like Fe XVIII, and the $2s^2 2p^4\ ^3P_2$-$2s 2p^5\ ^3P^o_2$ resonance transition in O-like Fe XIX. Deduced oscillator strengths are in good agreement with relativistic calculations. Tentative identifications are proposed for neonlike Fe XVII.

I. INTRODUCTION

The development of high-temperature plasmas for fusion gave rise to a considerable interest in the spectroscopy of highly ionized atoms. The data needs are particularly important for the transitions between low-lying states which involve no change in principal quantum number ($\Delta n = 0$). Among elements, iron is favored because stainless steel as a material for tokamak's walls is responsible for highly ionized impurities largely contributing to radiative energy losses. Results on multicharged Fe can also aid in the interpretation of astrophysical observations. Really the first laboratory studies of the spectra of Fe XVI to Fe XXIV have become most intensive following observation of the lines in the spectra of solar flares.

Very few beam-foil studies exist for intermediate[1] and very high[2] stages of ionization of iron. Highly charged iron spectra have only been surveyed at Tandem Van de Graaff energies by Bashkin *et al.*[3] with a poor counting rate and a wavelength resolution insufficient to allow unambiguous identifications and any lifetime measurement. For these reasons we have chosen to study the beam-foil spectra of iron at ~1 MeV/A in the far vacuum ultraviolet range with the good spectral and spatial resolution allowed by the relatively high-beam currents of a heavy-ion linear accelerator. Spectra of Fe XVI to Fe XX have been identified and lifetimes and oscillator strengths have been measured especially in the sodiumlike Fe XVI with a simple structure but with an unusually difficult experimental situation and for resonance transitions in higher stages of ionization where relativistic corrections may be of interest.

II. SPECTROSCOPY

Fe^{6+} beams are produced at 1.16 MeV/nucleon energy by the linear injector of the Orsay hybrid heavy-ion accelerator ALICE. Currents for the 8-mm diameter beam were of the order of 5×10^{11} particles/sec. After stripping through a 20 $\mu g/cm^2$ carbon foil, the charges present in the beam are mainly 14+ to 19+ (Fig. 1). This charge distribution is reflected by the relative intensities of the Fe XV to Fe XX 4–5 transitions as observed between 103 and 180 Å (Fig. 2). Light from a beam length of 0.5 mm is viewed through a 50 μm-wide slit of a 2-m Hilger grazing incidence spectrometer equipped with a Bendix S3029 X channeltron detector. With a spectral resolution of 0.5 Å, the hydrogenic 4–5 lines are only resolved for the single valence electron ion Fe XVI. The peaks 4–5 and 5–6 observed in Fe XVII to Fe XX are broadened to more than 1.2 Å. In spite of the uncertainties in the calculated wavelengths obtained by applying the polarization formula of Edlen[4] (uncertainties due to the spread of published polarizability values),[5-7] the identification of these lines is quite definite. The width of the 4–5 and 5–6 Fe XVII-Fe XX is due to the proximity of the different $(n, l \rightarrow n+1,\ l+1)$ lines for higher charges and the blending of the different terms.

Beam-foil spectra were more accurately recorded between 90 and 150 Å (Fig. 2), in the wavelength range of the inner-shell transitions $2s^2 2p^k$-$2s 2p^{k+1}$ in Fe XVIII, XIX, and XX ($k = 5$, 4, and 3) of astrophysical importance (solar flares)[8,9] and in the vicinity of the low-lying multiplets $3p$-$3d$ and $3s$-$3p$ of sodiumlike Fe XVI, around 260 and 350 Å, respectively (Fig. 3). To reduce the background in the short-wavelength part of the spectrum, the stray electrons were biased out by an additional electron suppressor plate.

To be free from Doppler-shifts correction, the wavelengths of observed peaks have been measured by reference to known lines in Fe XVI-Fe XX (Refs. 10 and 11). Blended peaks were deconvoluted by a Gaussian profile program. We believe the accuracy of our wavelengths to be about 0.1 Å for strong pure lines and 0.2 Å for weak

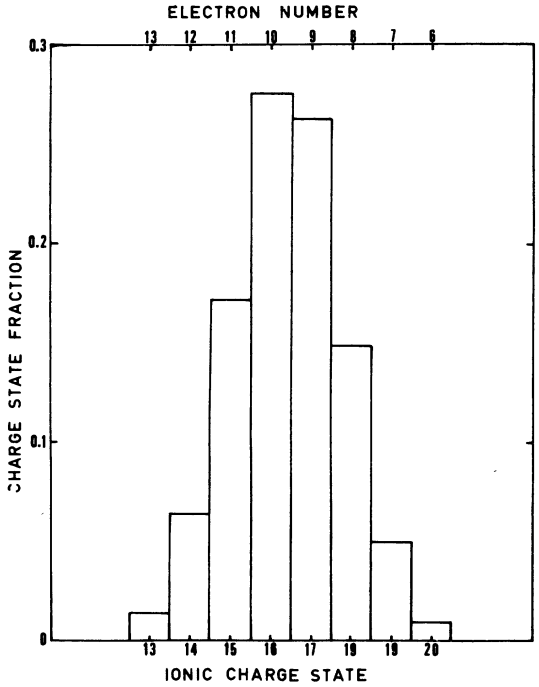

FIG. 1. Charge state distribution of a 1.16 MeV/A iron beam after transmission through a thin carbon foil.

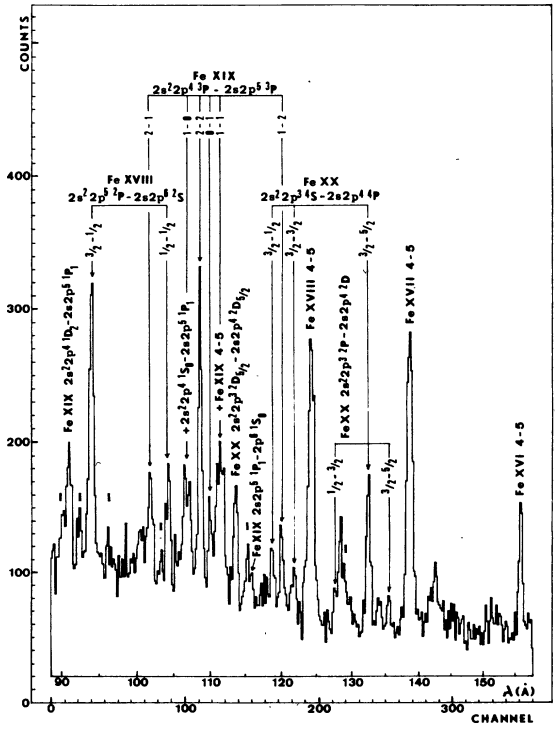

FIG. 2. Spectrum of foil-excited iron beam at 65 MeV between the wavelengths 90 and 160 Å. The linewidth is less than 0.5 Å full width at half maximum (FWHM). Heavy typed bars point out peaks tentatively identified to Fe XVII lines in Table I.

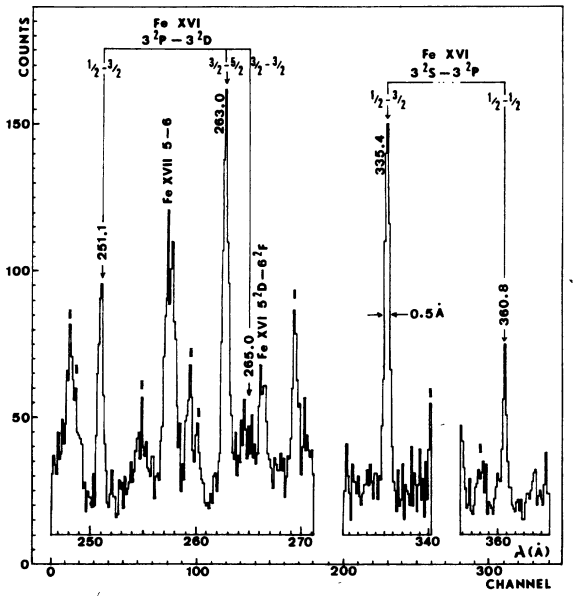

FIG. 3. Portions of a far ultraviolet spectral scan of a 65-MeV foil-excited iron ion beam. Components of $3s$-$3p$ and $3p$-$3d$ multiplets are well resolved and free of any blending. Heavy typed bars point out peaks tentatively identified to Fe XVII lines in Table I.

or blended lines. Results of beam-foil spectra are in good agreement with the spectra from spark source and laser induced plasma of Doschek *et al.*[12] in Fe XVIII to Fe XX and Kononov *et al.*[13] in Fe XX.

Measured intensities of the strong-multiplet components in Fe XVIII and Fe XIX are approximately distributed as calculated in *LS* coupling and as given by Fawcett[14] in intermediate coupling (to ~15%).

More tentative is the identification of neonlike Fe XVII lines which have to be present in these spectra: The charge 16^+ is the most probable one at the Linac energy and the $2s^22p^53l$-$3l'$, $2s2p^63l$-$3l'$, and $2s^22p^53l$-$2s2p^63l$ transitions of Fe XVII cover the recorded wavelength ranges. Recently Bogdanovich *et al.*[15] computed the energies of $2s^22p^53l$ and $2s2p^63l$ configurations in the neon isoelectronic series by two methods: First, in the Hartree-Fock approximation and second, according to the first-order perturbation theory (PT) with relativistic corrections via the Breit operator. There are large discrepancies between the two methods and with the previous calculation of Loulergue and Nussbaumer.[16] However, a comparison with experimentally known lines shows a better agreement with the Bogdanovich PT computations of energies. Calculated transition probabilities of Loulergue[16] and Crance[17] were used to select presumably stronger lines. Within these

TABLE I. Tentative identifications in Ne-like Fe XVII.

Expt. wavelength (Å)	Theor.[a] wavelength (Å)	Transitions
90.3	90.56	$2s^22p^53d\,^3F_4$-$2s2p^63d\,^3D_3$
	90.64	$3p\,^3S$ - $3p\,^3P_0$
92.4	92.40	$3p\,^3D_3$- $3p\,^3P_2$
96.1	96.07	$3p\,^1D_2$- $3p\,^3P_1$
102.8	102.79	$3p\,^1P_1$- $3p\,^3P_0$
	102.40	$3d\,^3F_0$- $3d\,^3D_2$
115.0	114.80	$3d\,^3D_3$- $3d\,^1D_2$
129.3	129.04	$3d\,^3F_3$- $3d\,^1D_2$
206.6	206.85	$2s^22p^53p\,^3D_2$-$2s^22p^53d\,^3F_3$
243.9	243.97	$3p\,^3S_0$ - $3d\,^3F_2$
244.8	244.81	$3p\,^3D_1$- $3d\,^3D_1$
248.5	248.69	$3s\,^3P_2$- $3p\,^3P_2$
249.3	249.44	$3s\,^3P_2$- $3p\,^3P_1$
254.0	252.09[b]	$3s\,^1P_1$- $3p\,^1S_0$
259.7	259.44	$2s2p^6\,3p\,^3P_1$-$2s2p^63d\,^3D_2$
260.3	260.33	$2s^22p^53s\,^3P_1$-$2s^22p^53p\,^3P_1$
269.6	270.33	$2s2p^6\,3p\,^3P_2$-$2s2p^63d\,^3D_3$
340.5	340.85	$2s^22p^53s\,^3P_1$-$2s^22p^53p\,^1D_2$
358.1	357.86	$3p\,^1P_1$- $3d\,^3F_2$

[a] Bogdanovich *et al.*, Ref. 15.

[b] Loulergue, in Ref. 16, gives the value 255.03 Å for this highly probable transition. With the experimental energy for the lower state and the PT energy for the upper state the wavelength becomes 254.46 Å.

assumptions all the theoretically strong transitions $2s3p$-$2p3p$ and $2s3d$-$2p3d$ have been observed if not blended, and peaks observed in our partial spectra around 250 and 350 Å can be identified with strong transitions $2p^53p$-$2p^53d$, $2p^53s$-$2p^53p$, or $2s2p^63p$-$3d$ of Fe XVII (Table I).

A few lines of the short wavelength portion of the spectrum remain unidentified. The strongest one we observe at 128.65 Å had also been found with a great intensity at 128.74 Å in solar-flare emission.[8] The assignment of this line and of weaker lines observed at 142.8 and 121.25 Å to the $(2s^22p^2$-$2s2p^3)\,^3P_0$-$^3D_1^o$, $^3P_1$-$^3D_2^o$, and $^3P_2$-$^3P_2^o$ transitions in Fe XXI (Ref. 13) is quite uncertain because the fraction of Fe^{20+} ion is very small in the beam at that energy (Fig. 1).

III. LIFETIMES AND OSCILLATOR STRENGTHS

The radiative lifetimes of all the levels in the $n=3$ manifold of Fe XVI, of the $2s2p^6\,^2S_{1/2}$ level in Fe XVIII, and of the $2s2p^5\,^3P_2$ level in Fe XIX were measured by using the beam-foil time-of-flight method. The acceptance angle of the monochromator defines a beam source length of 0.5 mm (time window 30 psec). Intensity decays were normalized to a fixed ion beam charge collected in a Faraday cup. The relative energy loss in the carbon foil was about 1% so that the postfoil ion velocity was 15 mm/ns, defined to better than 1%.

A. Oscillator strengths of the 3s-3p and 3p-3d transitions in sodiumlike Fe XVI

The partial energy level scheme of Fe^{15+} (Fig. 4) shows the $\Delta n=0$, $n=3$ transitions and a number of cascades from higher "yrast" levels. Although the $3p$ lifetimes are two or three orders of magnitude longer than their close-lying cascades, the recorded decay curves show long tails (Figs. 4 and 5). These slow decays are mainly due to repopulation of $n=3$ levels by the high l ($l=n-1$) states with $n>10$ cascading to $3d$ via the intermediate

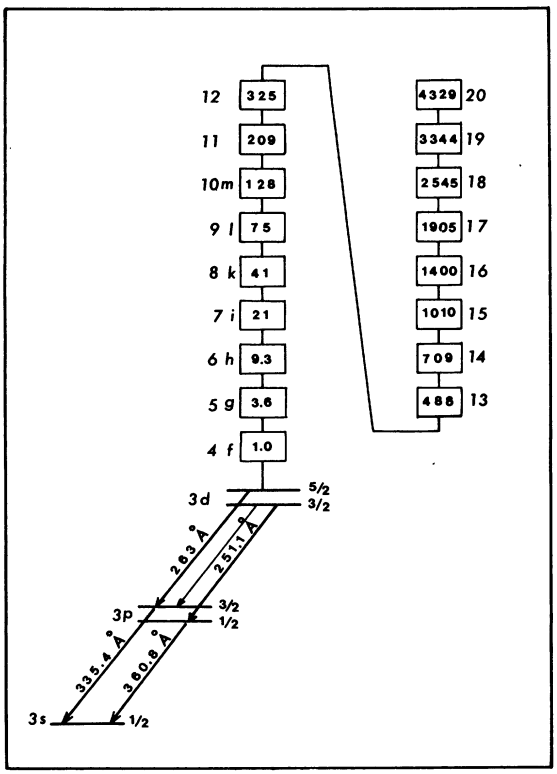

FIG. 4. Partial energy level diagram showing in-shell transitions within the $n=3$ manifold of Fe^{15+} and the yrast cascades included in the computer simulated decay curves of Figs. 5 and 6. The boxed numbers are the hydrogenic values for level lifetimes (psec).

yrast unbranched chain. We are in the unusually difficult experimental situation of the $\Delta n=0$ transitions in Na I (Ref. 18) and Cu I (Ref. 19) isoelectronic sequences.

We first analyzed the decay curves by the usual multiexponential fitting technique. As this approach may be inadequate here, we completed the data analysis by two other independent methods. The $3p\,^2P_{3/2}$ transition to the ground state was studied by a derivative method using both the $3s$-$3p$ and $3p$-$3d$ decays. Assuming that the whole cascade repopulation of $3p$ levels comes via the $3d$ levels, the lifetime

$$\tau_{3p}=\frac{kI_{3d}(t)-I_{3p}(t)}{\frac{d}{dt}I_{3p}(t)}$$

is obtained as a function of the unknown normalization parameter k. $I_{3p}(t)$ and $I_{3d}(t)$ are the observed intensities of the light emitted by the $3s$-$3p$ and $3p$-$3d$ transitions and $k=k'/\tau_{3d}$ where k' is a calibration factor taking the spectral efficiency of the optical device into account. By varying k, it is possible to get with a good approximation, a constant value for τ_{3p} which is the real value for the $3p$ level lifetime. An important advantage of the technique is the cancellation of the backgrounds.

In order to gain a better understanding of cascade effects we undertook a study of their importance by way of a computer simulation of beam-foil decay curves. To perform such a simulation we used theoretical values for the transition probabilities along the yrast chain and two different models for the relative initial populations of the cascades states with respect to the primary levels. The higher-lying level lifetimes very well approach the hydrogenic values [divided by $(Z-10)^4$]. It is already true for $4f$ as shown by the comparison with the result obtained from a Coulomb approximation.[20] Figure 4 gives the theoretical lifetime values used in the simulations. The most critical piece of data is the lifetime for the primary level ($3p$ or $3d$) and the choice for the initial populations. The level distribution after beam-foil excitation is not well known, especially for heavy ions. The population model $(2l+1)n^{-k}$ was applied for $k=2$ and 3. A rectangular instrumental resolution function 30 psec wide was convoluted with the theoretical de-

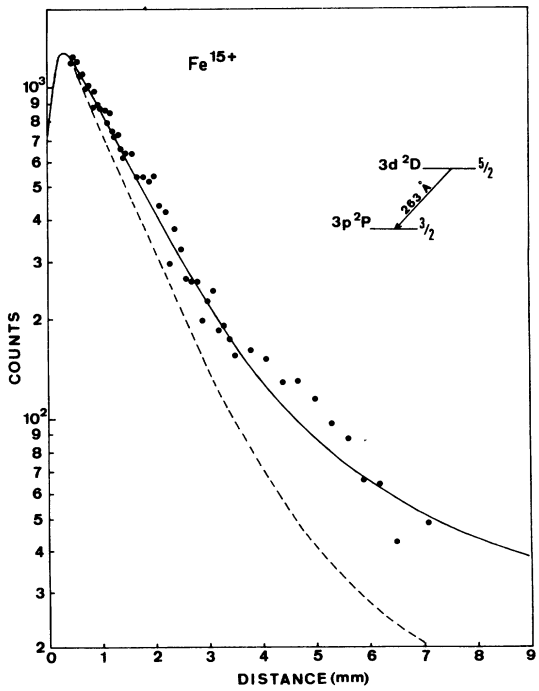

FIG. 5. Spatial decay-in-flight curve for the $3d\,^2D_{5/2}$ state in Fe XVI. Experimental data are represented by full points and computer simulations by a full line for the population distribution $(2l+1)n^{-2}$ and by a dashed line for the population distribution $(2l+1)n^{-3}$. A rectangular instrumental resolution 0.5 mm wide (30 psec) has been convoluted with the theoretical decay.

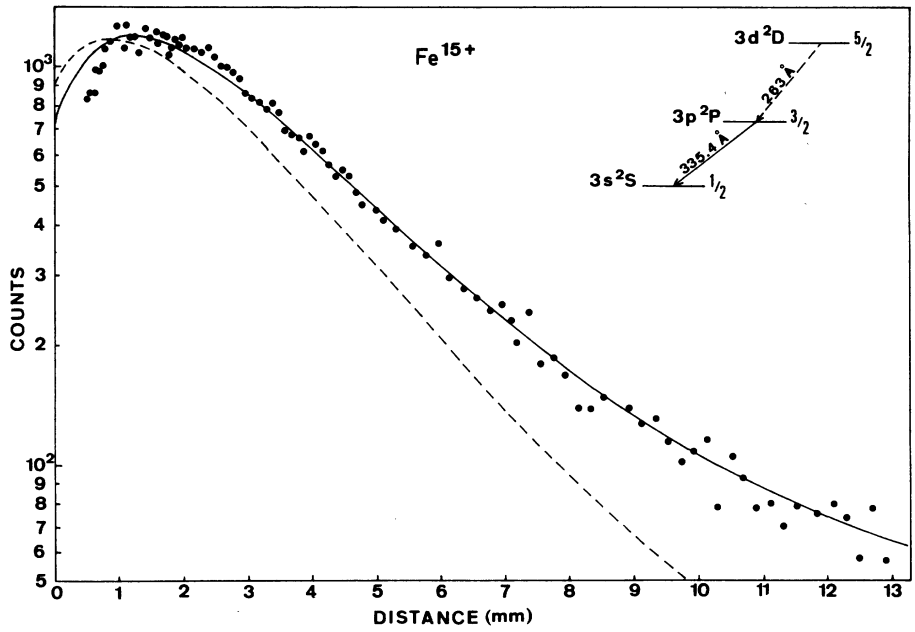

FIG. 6. Same as in Fig. 5 except upper state $3p^2P_{3/2}$.

cay curves. The $(2l+1)n^{-2}$ population model achieves a good fit with plausible lifetimes for $n=3$ levels, far superior to the $(2l+1)n^{-3}$ model (Figs. 5 and 6). Such a result has been recently found in the intensity decay for the foil excited $4P_{3/2}$ state in copperlike Kr VIII (Ref. 21) but, at the present time, only a few cases have been analyzed with such a procedure and the situation

TABLE II. Mean lives and oscillator strengths in sodiumlike Fe XVI. The bracketed numbers are the lifetime values for cascading $3d$ levels as issued from the exponential-fit program.

Wavelength (Å)	Transition	Mean life (psec) This expt.	Mean life (psec) Theory d	Oscillator strength This expt.	Oscillator strength Theory Line[d]	Oscillator strength Theory Multiplet
251.1	$3p\,^2P^o_{1/2}$-$3d\,^2D_{3/2}$	55±4[a];66.8[b]	54.4	<0.344[a]	0.293	
				<0.283[b]		
						0.282[d];0.264[e];0.288[f]
263.0	$3p\,^2P^o_{3/2}$-$3d\,^2D_{5/2}$	62±5[a];82.8[b]	61.9	0.251[a]	0.251	
				0.188[b]		
335.4	$3s\,^2S_{1/2}$-$3p\,^2P^o_{3/2}$	125±10[a]	124.4	0.270[a]	0.271	
		128±6 (68)[b]		0.263[b]		
				0.244[c]		
						0.395[d];0.370[e];0.370[f]; 0.359[g]
360.8	$3s\,^2S_{1/2}$-$3p\,^2P^o_{1/2}$	155±10[a]	157.4	0.126[a]	0.124	
		157±10		0.124[b]		

[a] From the simulation procedure.
[b] The three exponential-fit program.
[c] The derivative method.
[d] Weiss, Ref. 22.
[e] Laughlin, Ref. 23.
[f] Biemont, Ref. 24.
[g] Froese Fisher, Ref. 25.

regarding the appropriate population model to be used is not clear.

Results for lifetimes obtained by the different methods of analysis are given in Table II, together with deduced oscillator strengths and comparison with theoretical values. The error bars given in Table II are based on the standard deviation for each separate decay curve fit. Our results for the $3p$ lifetimes are consistent within $\pm 5\%$ whatever the methods used to analyze the experimental decays. However, the data for the $3d$ levels clearly demonstrate the inadequacy of the usual multiexponential fitting technique for analyzing these levels strongly repopulated by yrast cascades, and the necessity to take a detailed account of the cascade scheme. The most important individual cascade curves for modifying the "linear" region, where the primary lifetime is usually determined, are the first ones with low n, $n \lesssim 8$ for $3d$ and $n \lesssim 10$ for $3p$. As the intensity of the $3d$-$3p$ and $3p$-$3s$ lines have been observed only along six or seven e-folding decay lengths of the primary level, it is sufficient to enter cascades from $n < 15$ yrast levels in the calculation program to simulate the whole experimental curves.

It can be seen from the Table II that good agreement exists between the present measured values of the lifetimes and oscillator strengths and the theoretical Hartree Fock (HF) calculations, especially those which include relativistic corrections, either directly as in Weiss,[22] or indirectly by using observed transition frequencies (more sensitive to relativistic effects than the transition matrix elements) as in Laughlin.[23]

Along the isoelectronic sequence $3p$-$3d$, the measured oscillator strengths of elements lighter than argon (Ref. 26) are inferior to the theoretical values. In the same way, the experimental lifetimes of Pegg *et al.*[27] for Ni XVIII $3d^2D_{5/2}$ and Cu XIX $3d^2D_{3/2}$ (after correction for the branching ratio) are 15 to 20% longer than the theories predict. The analyzing procedure used was always a multiexponential fit. Experimental lifetimes of $3p^2P$ levels are more consistent with all theories.

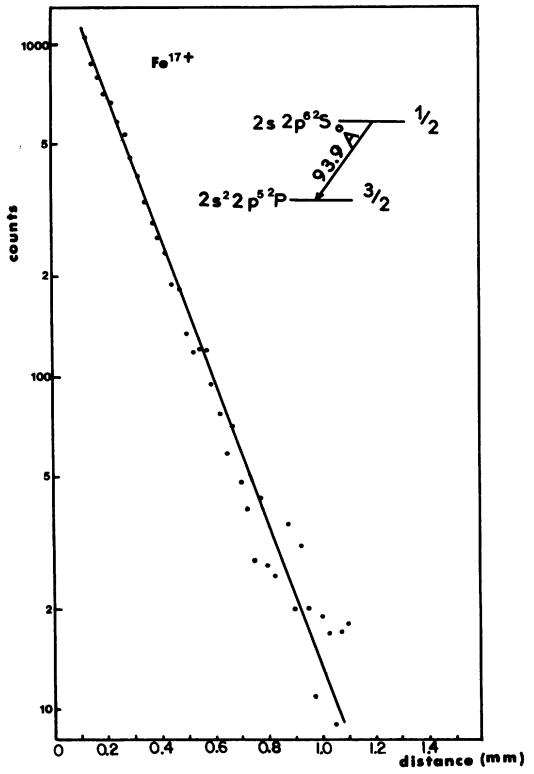

FIG. 7. Decay curve of the $2s^22p^5\,^2P_{3/2} - 2s2p^6\,^2S_{1/2}$ transition of Fe XVIII, after subtraction of background. The semilog plot is seen to be linear for ~70 psec which is equivalent to approximately six decay lengths.

TABLE III. Mean lives in Fe XVIII and Fe XVI.

Wavelength (Å)	Transition	Mean life (psec) This expt.	Theory
Fe XVIII			
93.9	$2s^22p^5\,^2P^o_{3/2}$-$2s2p^6\,^2S_{1/2}$	12.2 ± 0.8	8.0[a];10.1[b];10.8[d];13.0[e]
Fe XIX			
108.4	$2s^22p^4\,^3P_2$-$2s2p^5\,^3P^o_2$	23.5 ± 2.0	17.8[a];22.5[c];22.7[d]; 29.4[e];22.1[f];20.8[g]

[a] Smith and Wiese, Ref. 30.
[b] Safronova *et al.*, Ref. 28.
[c] Safronova *et al.*, Ref. 29.
[d] Sinanoğlu, Ref. 27, from f values and experimental wavelengths.
[e] From theoretical transition probabilities of Sinanoğlu, Ref. 27.
[f] Doschek *et al.*, Ref. 12, from $gf(^3P_2$-$^3P_2)$ and LS coupling.
[g] Fawcett, Ref. 14, from $gf(^3P_2$-$^3P_2)$ and $(^3P_1$-$^3P_2)$.

B. Mean life measurement of Fe XVIII $2s2p^6\ ^2S$ and Fe XIX $2s2p^5\ ^3P_2$

The studied transitions are the strongest ones we observed between $n=2$ levels in F- and O-like iron ions. The lifetimes of these levels are shorter than the detection window determined in the whole experiment by the fixed slit width of the monochromator. This wide window is relatively advantageous for long-lived decay components and tends to rub out the fast decays.

In spite of this enhancement of the apparent replenishment ratio from long cascades, the decay curve of Fe XVIII $2s2p^6\ ^2S_{1/2}$ is almost rigorously mono-exponential along the 1.1-mm observation path (~6 mean lives). That means that the cascades on this level are very weak. In fact there are no levels within L shell allowed to transit to the $2s2p^6\ ^2S$. Furthermore no $2s2p^5nl$ $(n \geq 3)$ are experimentally known in the energy diagram. In the error bar of the experimental $2s2p^6\ ^2S$ mean life (Table III) statistical uncertainties associated with the decay curve fitting process, mainly by assuming cascades or not, are included in addition to 1% systematic uncertainties on the beam velocity and the beam-charge normalization (Fig. 7).

The Fe XIX $2s2p^5\ ^3P_2$ decay is more difficult to analyze because the deduced mean life is very sensitive to the background and cascade corrections. The mean life (Table III) is obtained from the experimental curves assuming that the long tails are only due to the background without any cascade. The quoted error bar is associated to uncertainties in this hypothesis. Another fit is possible with comparable mathematic confidence assuming very heavy cascades. It leads to a mean life shortened by about 25%. We rejected this last analysis as physically very improbable.

The experimental mean life of Fe XVIII $2s2p^6\ ^2S$ would be in agreement with the non-closed-shell many electron theory (NCMET) calculation of Sinanoğlu.[28] However, it is about 15% higher than the NCMET value corrected by experimental wavelength, and the Safronova's many-body perturbation calculation.[29]

Our determination of the Fe XIX $2s2p^5\ ^3P_2^o$ agrees with the Safranova's Z-expansion calculation,[30] which includes relativistic effects, and with the gf value of Doscheck. To be consistent with our experimental result the nonrelativistic NCMET transition probability of Sinanoğlu[28] has to be corrected for relativistic energies by using experimental wavelengths. The 15% difference between our results and Fawcett's gf values[14] is consistent with the claimed accuracy of his data in intermediate coupling using *ab initio* calculation of Cowan and empirically derived values. Older f values presented by Smith and Wiese[31] are evidently too high for both electronic sequences.

[1] P. D. Dumont, Y. Baudinet-Robinet, H. P. Garnir, E. Biemont, and N. Grevesse, Phys. Rev. A 20, 1347 (1979).

[2] D. D. Dietrich, J. A. Leavitt, S. Bashkin, J. G. Conway, H. Gould, D. Mac Donald, R. Marrus, B. M. Johnson, and D. J. Pegg, Phys. Rev. A 18, 208 (1978).

[3] S. Bashkin, J. A. Leavitt, D. J. Pisano, K. W. Jones, P. M. Griffin, D. J. Pegg, I. A. Sellin, and T. H. Kruse, Nucl. Instrum. Methods 154, 169 (1978).

[4] B. Edlen, in *Handbuch der Physik*, *XXVII*, *Spectroscopy* 1 (Springer, Berlin, 1964); Phys. Scr. 19, 255 (1979).

[5] S. O. Kastner and M. L. Wolf, J. Opt. Soc. Am. 69, 1279 (1979).

[6] P. Vogel, Nucl. Instrum. Methods 110, 241 (1973).

[7] V. P. Shevelko and A. V. Vinogradov, Phys. Scr. 19, 275 (1979).

[8] S. O. Kastner, W. M. Neupert, and M. Swartz, Astrophys. J. 91, 261 (1974).

[9] K. P. Dere, Astrophys. J. 221, 1062 (1978).

[10] R. L. Kelly and L. J. Palumbo, *Atomic and Ionic Emission Lines below 2000 Angströms* (Naval Research Laboratory, Washington, D. C., 1973).

[11] J. Reader and J. Sugar, J. Phys. Chem. Ref. Data 4, 353 (1975).

[12] G. A. Doschek, U. Feldman, R. D. Cowan, and L. Cohen, Astrophys. J. 188, 417 (1974); G. A. Doschek, U. Feldman, J. Davis, and R. D. Cowan, Phys. Rev. A 12, 980 (1975); U. Feldman, G. A. Doschek, R. D. Cowan, and L. Cohen, Astrophys. J. 196, 613 (1975).

[13] E. Ya. Kononov, K. N. Koschelev, L. I. Podobedova, S. V. Chakalin, and S. S. Churilov, J. Phys. B 9, 565 (1976).

[14] B. C. Fawcett, At. Data Nucl. Data Tables 22, 473 (1978).

[15] P. U. Bogdanovich, Z. B. Rudzikas, V. I. Safronova, and S. D. Shadzhyuvena, Opt. Spectrosk. 44, 1054 (1978) [Opt. Spectrosc. (USSR) 44, 618 (1978)].

[16] M. Loulergue and H. Nussbaumer, Astron. Astrophys. 45, 125 (1975).

[17] M. Crance, At. Data 5, 186 (1973).

[18] R. J. Crossley, L. J. Curtis, and C. Froese Fischer, Phys. Lett. 57A, 220 (1976).

[19] W. L. Wiese and S. M. Younger, J. Phys. (Paris) Colloq. C 1, 146 (1979).

[20] A. Lindgård and S. E. Nielsen, At. Data Nucl. Data Tables 19, 533 (1977).

[21] A. E. Livingston, L. J. Curtis, R. M. Schectman, and H. G. Berry, Phys. Rev. A 21, 771 (1980).

[22] A. W. Weiss, J. Quant. Spectrosc. Radiat. Transfer 18, 481 (1977).

[23]C. Laughlin, M. N. Lewis, and Z. J. Horak, Astrophys. J. 197, 799 (1975).
[24]E. Biemont, J. Quant. Spectrosc. Radiat. Transfer 15, 531 (1975).
[25]C. Froese Fisher, in *Beam-Foil Spectroscopy*, edited by I. Sellin and D. J. Pegg (Plenum, New York, 1976).
[26]H. G. Berry, J. Désesquelles, P. Tryon, P. Schnur, and G. Gabrielse, Phys. Rev. A 14, 1457 (1976).
[27]D. J. Pegg, P. M. Griffin, B. M. Johnson, K. W. Jones, and T. H. Kruse, Astrophys. J. 224, 1056 (1978); D. J. Pegg, P. M. Griffin, B. M. Johnson, K. W. Jones, J. L. Cecchi, and T. H. Kruse, Phys. Rev. A 16, 2008 (1977).
[28]O. Sinanoğlu, Nucl. Instrum. Methods 110, 193 (1973).
[29]V. I. Safronova, J. Quant. Spectrosc. Radiat. Transfer 15, 231 (1975).
[30]V. I. Safronova, J. Quant. Spectrosc. Radiat. Transfer 15, 223 (1975).
[31]M. W. Smith and W. L. Wiese, Astrophys. J. Suppl. Ser. 23, 103 (1971).